OPTOELECTRONICS AND ADVANCED MATERIALS – RAPID COMMUNICATIONS Vol. 12, No. 5-6, May-June 2018, p. 275 - 278

Precise selection of focal length of manufacture graded-index planar microlens by simulation

M. KAVOSH TEHRANI*, R. TOFIGH MOVALU

Institute of Optics and Laser, Malek ashtar University of Technology, Shahin Shahr, Postal Code: 83145/115, Iran

In this paper, for exact determination of focal length in graded-index planar microlens (GRIN PML) after manufacturing, the procedure is as follows: At first, propagation of Gaussian beam in single and stacked graded-index planar microlens was simulated by optiwave software. By using simulation data, the focal length and beam width in focal point were obtained. Simulations showed that there is a linear relation between focal length and length of substrate. As a result, by choosing the optimum length of substrate we managed to obtain the arbitrary focal length of GRIN PML. In addition, we showed that beam width and focal length of stacked GRIN PML were less than GRIN PML.

(Received July 12, 2017; accepted June 7, 2018)

Keywords: Beam width, Focal length, Gaussian beam, Graded-Index Planar Microlens

1. Introduction

Graded-Index Planar MicroLens (GRIN PML) is made in an ion exchange process. The ion -exchange method is the most powerful technique due to its simplicity and flexibility in choosing the numerical aperture and dimensions. In ion exchange process, a piece of lithographic glass is inserted in a molten salt bath for certain duration at a certain temperature. The extent to which the diffusion speed can be increased depends on the following: (1) electric field strength, (2) ionic mobility, (3) glass constituency, (4) temperature, and (5) ionic source concentration. The refractive index can be increased or decreased as a result of a combination of two major effects, the first of which is related to the atomic size of the exchanging ions, and the second one is related to the electronic polarizability of the exchanging ions. Features of these GRIN PMLs include Planar Faces, less aberration than conventional lenses, angular characteristics, convenient focal lengths and numerical apertures, convenience of mounting and alignment. For these reasons, they are widely used in optical communication systems such as information processing and imaging systems [1-3]. Since light wave components are composed of a tandem lens waveguide, many of the components such as directional couplers, wavelength multiplexers, optical taps, etc., can be made with a 2-D configuration. If we use a 2-D array of holes, we can align optical fibers in a single batch process; and this facilitates mass production with easy alignment of optical circuits. Optical devices such as half mirrors and dielectric multilayer filters are easily introduced into the components [4-6].

We need to develop this type of micro-optic elements in different devices. The main problem in the ion exchange process is reaching a certain focal length after this process; however, we do not reach a proper focal length after making microlens.

In this work, a new simulation is presented for the propagation of Gaussian beam in a GRIN PML and Stacked Planar Optics by Optiwave software and the focal length and beam width in focal point using the simulations calculated and compared. With the simulation, we show there is a linear relationship between the substrate and the focal length. As a result, we can reach an arbitrary focal length by selecting a proper substrate length.

2. Refractive index profile model

Nowadays, the gradual refractive index is a great advantage in optical systems. Although the maximum refractive index changes will be limited to less than 0.27, this small change can lead to very useful results. The refractive index can be increased or decreased as a result of a combination of two major effects, the first of which is related to the atomic size of the exchanging ions. If a small ion such as Li^+ in the molten salt replaces a larger ion such Na^+ or K^+ in glass, the glass network will collapse around the smaller ion to produce a more densely packed structure that usually has a higher refractive index. Conversely, if a larger ion replaces a smaller one, the network expands to a less packed structure, yielding a lower refractive index. The second effect is related to the electronic polarizability of the exchanging ions. If an ion of larger electronic polarizability such as Ag^+, Cs^+, Tl^+, Rb^+ or K^+ replaces an ion of smaller polarizability such as Na^+, an increase in the refractive index will result, and vice versa.

After lens making, there are several methods such as interfering method [7], refracted near-field method [8], reflection method [9], imaging method [10] and near-field scanning method [11] for determining refractive index profile. In several articles, manufacturing methods [12-14], calculating the refractive index profile [15-17] and beam propagation in the medium with graded index [18, 19] have been investigated.

In manufacturing of graded-index planar microlens, if the exchange time of ions between composition and substrate be long, the shape of the ion penetration in the substrate will be almost hemispherical. Consequently, the shape of the concentration changes or, in other words, the gradual refractive index profile also has a spherical function.

In order to show how we can reach the exact focal length of GRIN PML after the manufacturing process, we have used a profile of GRIN PML provided by Nippon Sheet Glass (NSG) Company. The gradient index profile of this microlens is determined by the interference microscopy method as expressed by Eq. (1) [20]:

$$n(r,z)^2 = n_0^2\left[\mathbf{1},(gz)^2,(gz)^4,(gz)^6\right] \times \begin{bmatrix} \mathbf{1} & \mathbf{-1} & \mathbf{1.5} & \mathbf{-1.3} \\ \mathbf{-1.8} & \mathbf{15.4} & \mathbf{-46.6} & \mathbf{37.8} \\ \mathbf{10.4} & \mathbf{-127.4} & \mathbf{375.8} & \mathbf{-286.2} \\ \mathbf{-24} & \mathbf{298.2} & \mathbf{-859.1} & \mathbf{612.4} \end{bmatrix} \begin{bmatrix} \mathbf{1} \\ (gr)^2 \\ (gr)^4 \\ (gr)^6 \end{bmatrix} \quad (1)$$

Where, n_0=1.714 is the refractive index at the center of the aperture on the lens surface, $g = 0.545mm^{-1}$ $(for\lambda = 1550nm)$ is a normalization constant that denotes the lens power, $r = \sqrt{x^2 + y^2}$ is the radius of the lens aperture, and z is the optical axis of GRIN PML. Fig. 1 shows a schematic illustration of a GRIN PML where the refractive index of substrate is 1.658 and the maximum refractive index change is 0.056.

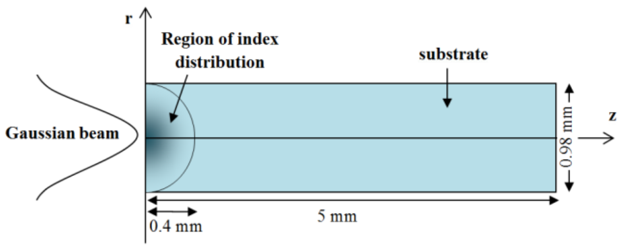

Fig. 1. Schematic illustration of a GRIN PML and its dimensions

The curves relevant to the refractive index expressed by equation (1) (for a micro-lens with hemispherical gradient index profile) in radial (z_{cut}=0) and axial (r_{cut}=0) directions, respectively, are shown in Figs. 2(a,b).

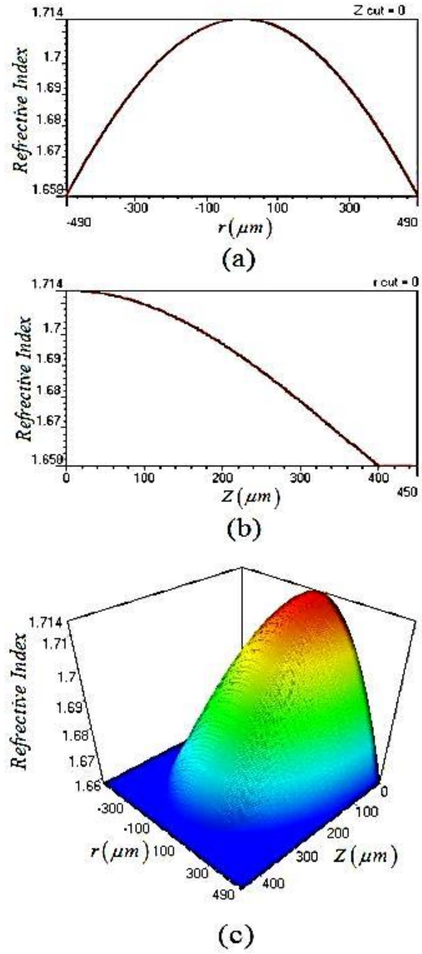

Fig. 2. (a) Refractive index changes versus radial coordinates in $z=0$; (b) Refractive index changes versus axial coordinates in $r=0$ (c). The three-dimensional graph of the refractive index

3. Simulation of Gaussian beam propagation in single microlens

Simulations for the propagation of the Gaussian beam are performed using the Optiwave software into a glass with refractive index changes according to relationship (1). According to Fig. 1, in this simulation, glass has the cross section of $0.98\,\mathrm{mm}\times 0.98\,\mathrm{mm}$ and length of 5 mm. The area of hemispherical index distribution has a diameter of 980μm and a maximum diffusion depth of 400μm . Glass surrounding medium is air. Fig. 3(a) shows the input intensity distribution of Gaussian beam to GRIN PML (with half width of 200μm and maximum intensity of 1 $W.m^{-2}$). Fig. 3(b) shows the intensity distribution of Gaussian beam after passing through the lens. By using this figure, the focal length can be obtained. Since the substrate length is 5 mm and maximum intensity is in position of 12.283 mm, the back focal length of GRIN PML will be 7.283 mm. The curve of radial intensity distribution at the focal point (z = 12.283 mm) is shown by Fig. 3(c). According to this figure, the beam width is

$32.88\mu m$, showing that this lens is usable in optical fibers. Fig. 3(d) shows the two-dimensional distribution of Gaussian beam intensity at the focal point (with maximum intensity of 10.16 $W.m^{-2}$).

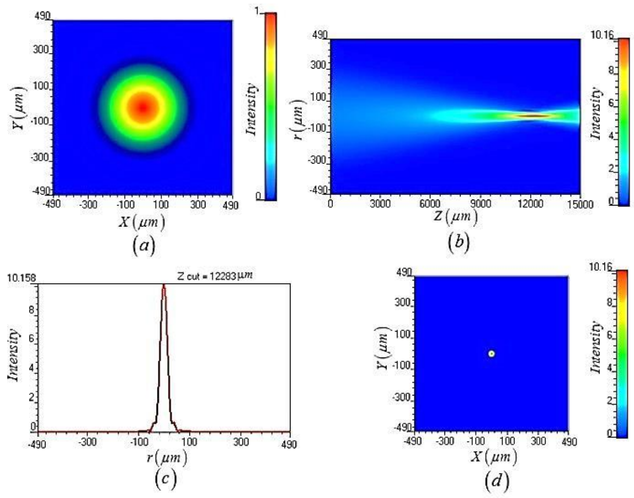

Fig. 3. (a) Input intensity distribution of Gaussian beam to GRIN PML in x-y cross section; (b) Two-dimensional intensity distribution of Gaussian beam in simulated area; (c) Intensity curve of Gaussian beam simulated in the focal point; (d) Intensity distribution of Gaussian beam focused by the GRIN PML in x-y cross section

4. Simulation of Gaussian beam propagation in stacked graded-index planar microlens

The stacked graded-index planar microlens is an array of two-dimensional waveguide. Here, Gaussian Beam Propagation through the stacked graded-index planar microlens has been simulated. First and second Length of lens, 2 and 5 mm, respectively, and its diameter of 0.98 mm are selected. Similar to the previous simulation, 2D-1D intensity distributions of the same Gaussian beam, when passing and after passing through the stacked graded-index planar microlens and also in focal point, are provided as shown in Figs. 4(a-d). According to these figures, the back focal length and beam width are obtained 1.377 mm and $17.34\mu m$, respectively. The simulations show that by using the stacked graded-index planar microlens, the focal length and the beam width of the GRIN PML can be reduced.

To make changes in the large refractive index during ion exchange process, the electric field is applied to the substrate [1]. The electric field is due to low mobility of some elements such as Tl^{+} is applied on the one hand to the other side of the substrate which causes the thermal penetration and mobility of most of the ions in the glass. The electric field applied to a very small aperture on the substrate often results in a hemispherical refractive index profile. But our goal in this paper is to simulate Gaussian beam propagation from a pre-made lens type and changing the length of the lens bed to obtain a specific focal length.

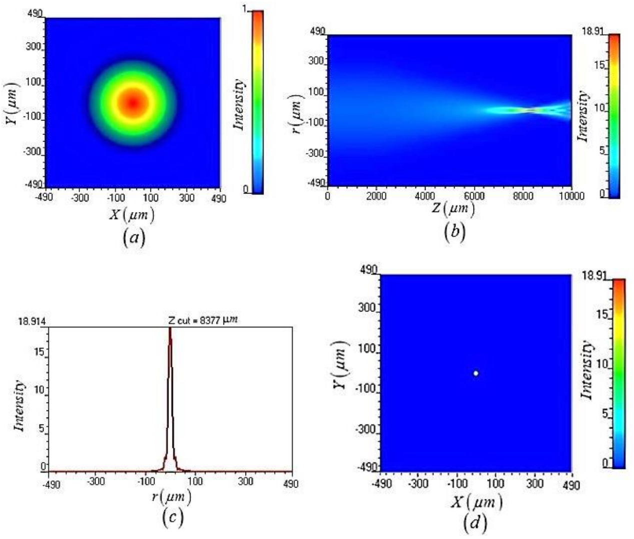

Fig. 4. (a) Input intensity distribution of Gaussian beam to stacked GRIN PML in x-y cross section; (b) Two-dimensional intensity distribution of Gaussian beam in simulated area; (c) Intensity curve of Gaussian beam simulated in the focal point (d) Intensity distribution of Gaussian beam focused by the stacked GRIN PML in x-y cross section

5. Selecting a certain focal length by choosing a proper substrate length

To select the specific focal length, all of the simulations are repeated for different lengths of substrate (l=2, 3, 4, 5, 6, 7, 8, 9 mm) when Gaussian beam is incident to front surface of single and stack gradient index region. The relevant results are listed in Table 1, 2.

Table 1. Simulation results of back focal length single GRIN PML

Substrate length (mm)	2	3	4	5	6	7	8	9
Effective focal length (mm)	11.95	12.04	12.15	12.28	12.35	12.46	12.55	12.62
back focal length (mm)	9.951	9.044	8.155	7.28	6.35	5.46	4.55	3.62
beam width at the focal point (μm)	32.88	32.88	32.88	32.88	32.88	32.88	32.88	32.88

Table 2. Simulation results of back focal length stacked GRIN PML

Substrate length (mm)	2&2	2&3	2&4	2&5	2&6
Effective focal length (mm)	8.080	8.189	8.377	8.385	8.484
back focal length from incident surface (mm)	4.080	3.189	2.377	1.385	0.484
beam width at the focal point (μm)	17.34	17.34	17.34	17.34	17.34

The curve of focal length in terms of substrate length for two cases is plotted in Fig. 5. According to this linear curve, to obtain the arbitrary focal length, one can determine the optimum length of the substrate.

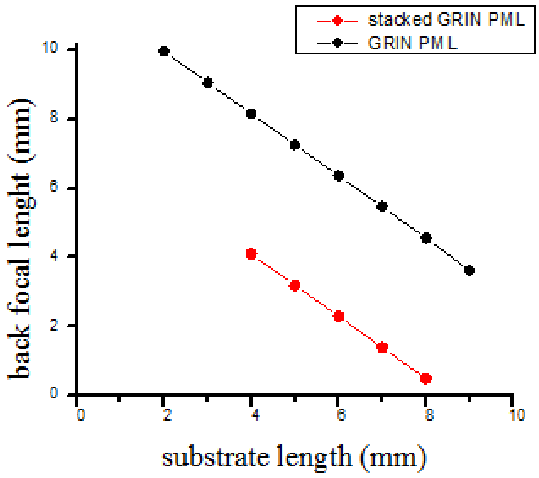

Fig. 5. Back focal length in terms of substrate length

6. Conclusion

In the present work, we showed that the relation between the substrate length and the focal length is linear for each of the two cases. Therefore, we can obtain the precise special focal length by determining the focal length in terms of substrate length by simulation and cutting of the end lens.

With regard to the fact that maximum variation in refract index happening by exchanging ion in glasses is 0.27, fabrication of microlense with short focal length is unreachable; however, by combining two microlenses, we can reach less than focal length and low beam width. Moreover, we showed that focal length and Gaussian beam width of stack Graded-Index microlenses decrease in comparison to single planar microlens approximately 5.8 mm and 15.54 μm respectively. Decrease in the focal length and Gaussian beam width increases the usability of the stack Graded-Index microlenses in a single mode fiber.

References

[1] A. I. Hernandez-Serrano, M. Weidenbach, S. F. Busch, M. Koch, E. Castro-Camus, JOSA B **33**(5), 928 (2016).
[2] J. Bähr, K. H. Brenner, Applied Optics **35**(25), 5102 (1996).
[3] S. Li, Y. Sun, J. Zhu, T. Tang, Optical Engineering **50**(11), 115001 (2011).
[4] Y. Kokubun, K. Iga, Applied Optics **21**(6), 1030 (1982).
[5] W. Singer, B. Dobler, H. Schreiber, K. H. Brenner, B. Messerschmidt, Applied Optics **35**(13), 2167 (1996).
[6] X. Sun, H. Ma, H. Ming, Z. Zheng, J. Yang, J. Xie, Optics & Laser Technology **36**(2), 163 (2004).
[7] I. P. Kaminow, J. R. Carruthers, Applied Physics Letters **22**(7), 326 (1973).
[8] M .Young, Applied Optics **20**(19), 3415 (1981).
[9] M. Ikeda, M. Tateda, H. Yoshikiyo, Applied Optics **14**(4), 814 (1975).
[10] X. Sun, H. Ma, H. Ming, Z. Zheng, J. Yang, J. Xie, Optics & Laser Technology **36**(2), 163 (2004).
[11] F. M. E. Sladen, D. N. Payne, M. J. Adams, Applied Physics Letters **28**(5), 255 (1976).
[12] J. Moisel, C. Passon, J. Bähr, K. H. Brenner, Applied Optics **36**(20), 4736 (1997).
[13] J. Nylk, M. V. Kristensen, M. Mazilu, A. K. Thayil, C. A. Mitchell, E. C. Campbell, S. J. Powis, F. J. Gunn-Moore, K. Dholakia, Biomedical Optics Express **6**(4), 1512 (2015).
[14] K. Iga, M. Oikawa, S. Misawa, J. Banno, Y. Kokubun, Applied Optics **21**(19), 3456 (1982).
[15] P. Haguenauer, J. P. Berger, K. Rousselet-Perraut, P. Kern, F. Malbet, I. Schanen-Duport, P. Benech, Applied Optics **39**(13), 2130 (2000).
[16] Y. Kokubun, T. Usui, M. Oikawa, K. Iga, Japanese Journal of Applied Physics **23**(1R), 101 (1984).
[17] M. Oikawa, K. Iga, T. Sanada, N. Yamamoto, K. Nishizawa, Japanese Journal of Applied Physics, **20**(4), L296 (1981).
[18] M. Oikawa, K. Iga, M. Morinaga, T. Usui, T. Chiba, Applied Optics **23**(11), 1787 (1984).
[19] X. F. Zhu, K. Iga, Applied Optics **25**(19), 3397 (1986).
[20] K. Iga, S. Misawa, Applied Optics **25**(19), 3388 (1986).

*Corresponding author: m_kavoh@mut-es.ac.ir